CHAPTER 2

Adriamycin-induced TNF-mediated CNS Toxicity: Insights into the Machanism of Chemobrain

Abstract

The clinical effectiveness of adriamycin (ADR), a potent chemotherapeutic, is known to be limited by severe cardiotoxic side effects. However, the effect of ADR on brain tissue is not well understood. It is generally thought that ADR is not toxic to the brain because ADR does not pass the blood-brain-barrier. The present study demonstrates that ADR autofluorescence was detected only in areas of the brain located outside the blood-brain barrier, but a strong tumor necrosis factor alpha (TNF) immunoreactivity was detected in the cortex and hippocampus of ADR-treated mice. Systemic injection of ADR led to a decline in brain mitochondrial respiration via complex I substrate shortly after ADR treatment (*$p<0.05$). Cytochrome c released and increased active-caspase 3 activity and TUNEL positive cell death. The levels of the known anti-apoptotic protein, Bcl-xL, and the pro-apoptotic proteins, p53 and Bax, were increased in mitochondria isolated from ADR-treated brain tissues. Furthermore, p53 migrated to mitochondria and interacted with Bcl-xL, supporting the hypothesis that mitochondria are targets of ADR-induced CNS injury. Neutralizing antibodies against circulating TNF completely abolished both the increased TNF in the brain and the observed mitochondrial injury in brain tissues. These results are consistent with the notion that TNF is an important mediator by which ADR induces central nervous system (CNS) injury. This study, the first to provide direct biochemical evidence of ADR toxicity to the brain, revealed novel mechanisms of ADR-induced CNS injury, and suggests a potential therapeutic intervention against circulating TNF-induced CNS effects.

Introduction

Adriamycin (ADR), an antibiotic produced by the fungus *Streptomyces peuctius*, is a potent anticancer drug commonly used in the treatment of a variety of cancers including breast cancer (Hitchcock-Bryan et al., 1986; Fisher et al., 1989). However, its clinical effectiveness is limited by the toxic effect on normal tissues (Singal et al., 1987, 2000; Meredith et al., 1983; Oteki et al., 2005), including a cumulative, dose-related cardiomyopathy (Singal et al., 1998). Recent studies in breast cancer survivors have shown persistent changes in cognitive function, including memory loss, tendency for distractions, and difficulty in performing multiple tasks, following chemotherapy (Schagen et al., 1999; Brezden et al., 2000). These studies report that cognitive deficits, particularly in the areas of memory and concentration, are associated with cancer chemotherapy regimens, both in the short-term after treatment, and up to 2 years and more than 5 years after diagnosis (Ahles et al., 2002; Ferrell et al., 1997). These cognitive problems, collectively called somnolence or cognitive dysfunction, are also reported in cancer patients undergoing adriamycin-based chemotherapy, especially breast cancer patients (Freeman et al., 2002; Schagen et al., 2001; Meyers CA., 2000).

Although the biochemical basis for these cognitive problems is unknown, it has been demonstrated that cancer therapeutic agents such as ADR can modulate endogenous levels of cytokines such as tumor necrosis factor alpha (TNF) (Usta et al., 2004). Enhanced circulating TNF can initiate local TNF production via activation of glia cells leading to production of reactive oxygen/nitrogen species (RONS) (Szelenyi, 2001). RONS, including superoxide, hydrogen peroxide, and nitric oxide, can react directly with each other or indirectly to generate even more reactive species (Halliwell and Gutteridge, 1999). We recently reported that seventy-two hours after a single i.p. injection of ADR, there was a significant increase in levels of protein oxidation and lipid peroxidation in brain tissues (Joshi et al., 2005). However, the mechanism by which ADR causes oxidative stress in the brain remains unknown.

It is well established that ADR does not cross the blood brain barrier (Bigotte et al., 1982a, 1982b), but that circulating levels of TNF can directly pass the blood brain barrier and activate microglia and neurons to further increase local TNF levels (Osburg et al., 2002). TNF is known to induce neuronal damage (Gutierrez et al., 1993). TNF-induced tissue injury is mediated, at least in

part, by its effect on mitochondria (Goossens et al., 1995). TNF induces morphologic damage of mitochondria and biochemical respiratory defects in cultured cells (Liu et al., 2004; Schulze-Osthoff et al., 1992). The cytotoxicity of TNF depends on the induction of the mitochondrial permeability transition pore (Lancaster et al., 1989). Thus, it is possible that an increase in TNF levels may be a link between ADR-induced oxidative stress and CNS injury.

The present study evaluated the relationship between ADR-induced TNF production, mitochondrial dysfunction, and CNS injury. The results provide biochemical insights into the mechanisms of ADR-induced CNS injury.

Materials and Methods

Animals: Eight-week-old male B6C3 mice (25-30g) were kept under standard conditions, and all experimental procedures were approved by the Institutional Animal Care and Use Committee of the University of Kentucky.

Treatments: Mice were injected in a single intraperitoneal (i.p.) dose of 20 mg/kg adriamycin (Doxorubicin hydrochloride, Gensia Sicor Phamaceuticals, Inc., Irvine, CA), or the same volume of saline as control for 3 h. This dose and time were based on previous studies in which we demonstrated ADR induced cardiomyopathy (Yen et al., 1996, 1999).

To determine whether the neutralization of TNF in the periphery would mitigate the brain biochemical effects of ADR, anti-mouse TNF antibody (R&D Systems, Minneapolis, MN) was diluted in saline and immediately injected in a single i.p. dose of 40 ng/kg, and anti-TNF antibody immediately followed by ADR also was injected to separate animals. Controls consisted of anti-TNF antibody alone or preimmune rabbit IgG or saline in the same total volume. All results were obtained from at least three separate experiments.

Localization of adriamycin in brain tissues

Mice were euthanized by the i.p. injection of 65 mg/kg of nembutal (Sodium pentobarbital, Abbott Laboratories, North Chicago, IL), and were perfused via cardiac puncture initially with 0.1 M phosphate buffered saline (PBS), pH 7.4, and subsequent fixation with 4% paraformaldehyde. Brain tissues were removed and coronal cryosection at regular intervals of 7-μm thickness was performed. The sections were prepared for immunohistochemistry and detection of ADR. ADR in brain tissue slices was directly visualized using an inverted fluorescence microscope (excitation filter 550 nm, and barrier filter 590 nm). Photomicrographs were taken with an Olympus MagnaFire digital camera (Olympus, America, Melville, NY).

Enzyme-linked immunosorbent assay (ELISA)

Mice were treated with 20 mg/kg ADR or saline as control. Blood samples were collected at 1, 3, 6, 9, 24 h and allowed to clot at 2-8^{O}C overnight. Serum samples were used to measure TNF levels, according to the mouse enzyme-linked immunosorbent assay following the manufacturers' instructions (mouse TNF-α/TNFSF1A immunoassay, R&D Systems, Minneapolis, MN). The TNF concentration in the sample was calculated from a recombinant mouse TNF standard curve. The minimum detection limit is typically less than 5.1 pg/mL.

Immunohistochemistry study

Brain tissue slices were fixed in 4% paraformaldehyde for 15 min, air dried, and washed with PBS. Non-specific proteins were blocked in blocking serum, consisting of 3% normal donkey's serum, and 0.3% Triton x-100 in PBS, and incubated at room temperature for 30 min. After blocking, slices were incubated with primary anti-TNF (Upstate, Lake Placid, New York), and anti-MAP2 antibody (Chemicon, Temecula, CA) was used as a neuronal marker, in order to study the location of TNF in neurons of cortical and hippocampal regions. The sections were kept in a humidified box at 4^{O}C overnight. Tissues were washed three times with PBS and then were incubated for 1 h with donkey antibody-conjugated secondary antibodies conjugated with fluorescent dyes. Excess secondary antibodies were removed by washing three times in PBS and once with deionized H_2O. Tissue slides were mounted with mounting medium (Vectashield, H-100, Vector Laboratories, Burlingame, CA). Photomicrographs were obtained using a Leica confocal fluorescence microscope (Leica Microsystems Inc., Bannockburn, IL, USA).

Mitochondrial isolation and purification

Mice were perfused via cardiac puncture with cold mitochondrial isolation buffer, the brain promptly removed, the cerebellum dissected away, and mitochondria immediately isolated from the freshly isolated brain by a modification of the method described by Mattiazzi et al. (2002).

Brain mitochondria were isolated in cold mitochondrial isolation buffer, containing 0.07 M sucrose, 0.22 M mannitol, 20 mM HEPES, 1 mM EGTA, and 1% bovine serum albumin, pH 7.2. Tissues were homogenized with a Dounce homogenizer and centrifuged at 1,500xg at 4^{O}C for 5 min before transferring the supernatants. The pellets were resuspended and centrifuged at 1,500xg at 4^{O}C for 5 min. The supernatants were combined and recentrifuged at 1,500xg at 4^{O}C for 5 min. The supernatants were separated and centrifuged at 13,500xg at 4^{O}C for 10 min. Mitochondrial pellets were resuspended in 50-100 μL cold mitochondrial isolation buffer. Protein concentration of isolated mitochondria was determined by the Bradford assay (Bradford, 1976). The final protein concentration was 20-40 mg/ml.

Mitochondrial respiration

Mitochondrial respiration was determined using Clark-type polarographic oxygen sensors (Hansatech Instruments, Kings Lynn, Norfolk, UK) to measure the rate of oxygen consumption. Freshly isolated mitochondria were suspended in respiration buffer at a concentration of 0.5 mg mitochondrial protein per mL of respiration buffer, which consists of 0.25 M sucrose, 50 mM HEPES, 1 mM EGTA, 10 mM KH_2PO_4, and 2 mM $MgCl_2$, pH 7.4. Oxygen consumption was measured with either pyruvate (10 mM) plus malate (10 mM) or succinate (10 mM) as substrates for respiration from complex I or complex II in the absence of exogenous ADP (state II) and after addition of 300 mM ADP (state III respiration). Rotenone (5 μM) was added to the reaction to inhibit respiration from complex I when succinate was used as the substrate. The ATPase inhibitor oligomycin (100 μg/mL) was added to inhibit mitochondrial respiration such that state IV respiration was similar to the state II respiration rate. FCCP (1 μM), an uncoupling agent, was added as a control of respiration. Respiration control ratios (RCR) were calculated as the ratios of state III and state II respiration as described previously by Estabrook (1967). The unit for state II rate and state III rate is nmole/min/mg protein.

Preparation of brain homogenate

Brains perfused with PBS were isolated, removed cerebellum and dissected from six groups of mice 3 h post injection of a single dose of ADR, anti-TNF antibody, anti-TNF antibody immediately followed by ADR, IgG or saline treated mice. Brain was isolated and placed in 0.1 M PBS, pH 7.4 containing protease inhibitors, 4 μg leupeptin, 4 μg pepstatin, and 5 μg aprotinin, washed and minced in ice-cold PBS containing protease inhibitors. Tissues were homogenized with a Dounce homogenizer and centrifuged at 12,500xg at 4^{O}C for 30 min before transferring the supernatant. Protein concentration of brain homogenate was determined by the Bradford assay (Bradford, 1976).

Western Blot analysis

Perfused brain homogenates and isolated mitochondrial proteins were separated via 12.5 % denaturing polyacrylamide gel electrophoresis (SDS-PAGE) and transferred to a nitrocellulose membrane. The membrane was blocked for 1 h at room temperature in blocking solution consisting of 5% non-fat dried milk, 0.5% Tween-20 and Tris-buffered saline (TBST), pH 7.9. After blocking, the membrane was incubated overnight at 4^{O}C with primary antibodies against TNF (Upstate, Lake Placid, New York) and β-actin (Clone AC-74, A5316, Sigma, Saint Louis, MI) in homogenate samples, or isolated mitochondria samples for p53 (Ab-11, Oncogene Research, Cambridge, MA), Bcl-xL (S-18), Bax (P-19), succinate dehydrogenase (SDHB) (Santa Cruz Biotechnology, Santa Cruz, CA), in blocking solution. The membrane was washed twice in TBST and incubated for 1 h with horseradish peroxidase-conjugated secondary antibodies in blocking solution. After incubation with secondary antibodies, the membrane was washed twice with TBST and once in TBS (TBS without 0.5% Tween-20). Immunoreactivities of the protein bands were detected by enhanced chemiluminescence autoradiography (ECL, Amersham Pharmacia Biotech, Arlington Heights, IL) as described by the manufacturer.

To further investigate cytochrome c release, mitochondrial and cytosolic fractions were isolated from brain tissues and were size separated and probed with anti-cytochrome c antibody

(BD Biosciences, CA). Succinate dehydrogenase (SDHB) and β-actin were used as loading controls employing the procedure described above.

Immunoprecipitation assays

Isolated mitochondrial protein (500 μg) was resuspended in 500 μL RIPA buffer (9.1 mM Na_2HPO_4, 1.7 mM NaH_2PO_4, 150 mM NaCl, 0.5% sodium deoxycholate, 1% v/v Nonidet P40, 0.1% sodium dodecyl sulfate, pH 7.2). Protease inhibitors (0.1 mg PMSF and 1 μg aprotinin per mL RIPA) were added at the time of use followed by incubation with 5 μg/ mL of mouse p53 antibody (Ab-11, Oncogene) at $4^{O}C$ overnight. Protein A/G-Agarose (50 μL) was added to the reaction mixture with the antibody. Immunocomplexes were collected by centrifugation at 1,000xg at $4^{O}C$ for 5 min, and then washed four times with RIPA buffer. Immunoprecipitated samples were recovered by resuspending in 2x sample loading buffer, and Bcl–xL (Santa Cruz Biotechnology, Santa Cruz, CA) proteins were detected by Western blot. IgG was used to immunoprecipitate the isolated mitochondrial protein and analysis of the pellet and supernatant by Western blot using antibody against Bcl-xL to exclude the interference from light chain. Immunoreactivity was evaluated on immunoblots by densitrometric analysis using a Bio-RAD densitometer (Bio-RAD Laboratory, Inc, Hercules, CA, USA).

Caspase 3 activity assay

Caspase 3 activity assay was performed with the use of a colorimetric substrate in accordance ith the protocol supplied by the manufacturer (Sigma, St. Louis, MO). In brief, mice were anesthetized and perfused with 1xPBS to reduce any enzyme activity associated with intravascular blood components. Brains were dissected and homogenized in lysis buffer containing 50 mM HEPES, pH 7.4, 5 mM CHAPS, 5 mM DTT plus 1 μg/mL aprotinin and pepstatin. The brain homogenates were incubated on ice for 15 min and centrifuge at 16,000xg for 10 min. The protein concentration was determined by the Bradford method and the caspase 3 activity in the supernatant was measured immediately. Fifty microgram protein samples or positive control in 10 μL were added

to 980 μL assay buffer. The reaction was initiated by adding 10 μL of 20 mM caspase 3 substrate Ac-DEVD-pNA. The tubes were covered and incubated at 37^{O}C over night. Cleavage of the chromophore from the substrate was detected spectrophotometrically at a wavelength of 405 nm.

TUNEL assay

The assay was performed following the manufacturer instructions (Promega, Medison, WI). Briefly, the cryosections of brain tissues were fixed with 4% paraformaldehide, permeabilized with Triton X-100, and incubated with biotinylated nucleotide and recombinant termination deoxynucleotidyl transferase (rTdT) for 1 h at 37^{O}C. The fragmented DNA labeled at the ends was coated with horseradish peroxidase-labeled streptavidin (stretavidin HRP) and was detected as dark brown condensed nuclei, a positive indication of cell death. The sections were counterstained with methyl-green, and were incubated 5 min in methyl green staining dye, rinsed in distilled water and dehydrated quickly through 95% alcohol (10 dips) and then 2 changes of 100% alcohol (10 dips each). Finally sections were cleared in xylene and mounted with mounting medium. Positive control samples were prepared by incubating sections with DNase I prior to treatment with terminal transferase. Negative controls consisted of specimens in which deoxynucleotidyl transferase was omitted.

Statistical analysis

Statistical comparisons were made using one-way ANOVA followed by Newman-Keuls multiple comparisons test. Data are expressed as mean + SEM.

Results

Adriamycin accumulation in brain tissues

To explore the possibility that ADR accumulates in brain tissue, mice were given 20 mg/kg ADR by a single i.p injection. ADR accumulation in the CNS was studied by direct ADR fluorescence in brain slices using an inverted fluorescence microscrope. The specific orange-red fluorescence of ADR was observed in several areas outside the blood brain barrier, including the choroid plexus as previously reported by Bigotte et al. (1982a, 1982b). ADR fluorescence was clearly distinguishable from the background of untreated control, but was not observed in cortex and hippocampus (Fig. 2.1). When anti-TNF antibody and ADR were injected into mice together, ADR fluorescence was still observed (Fig. 2.1B). Fluorescence was not observed in mice treated with anti-TNF antibody alone (Fig. 2.1C).

Adriamycin-induced circulating TNF levels

TNF levels in serum were significantly higher in mice treated with ADR than those from controls (*$p<0.001$, Fig. 2.2). The increased TNF levels were detectable as early as 1 h and were sustained throughout a 24 h period after ADR treatment.

Increased TNF level in brain tissues

TNF levels were significantly increased in brain tissue homogenates as detected by Western blot analysis, following administration of ADR (Fig. 2.3). Anti-TNF antibody blocked ADR-mediated increased brain levels of TNF (Fig. 2.3). However, non-specific IgG was unable to block ADR-induced TNF elevation in brain (Fig. 2.3). To determine the localization of TNF in brain tissues, tissue slices were stained with anti-TNF and anti-MAP2 antibodies to localize TNF. The TNF levels clearly were increased in neurons of cortex and hippocampus compared with saline controls, since MAP2 is a neuron-specific marker (Fig. 2.4 and 2.5). To verify that the observed TNF in the

brain was mediated by ADR-induced circulating TNF, we co-injected a neutralizing antibody against TNF along with ADR. The increased levels of cortical and hippocampal or brain homogenate TNF were blocked in mice treated with anti-TNF antibody and ADR.

Adriamycin-induced mitochondrial dysfunction

To investigate the effect of ADR on brain mitochondrial function, brain mitochondrial respiration using pyruvate plus malate and succinate as the substrates was measured. The data are presented as the RCR of each treatment group and the IgG or saline-treated control group from each set of experiments. As shown in Fig. 2.6, the values of RCR from state III and state II respiration, via complex I but not complex II (data were not shown), were significantly decreased in the ADR or IgG followed by ADR-treatment group compared to controls (*$p<0.05$). In mice treated with anti-TNF antibody only, or in mice treated with anti-TNF antibody followed by ADR, brain mitochondrial respiration was not significantly different from that of the control group. Taken together, these results indicate that ADR-induced circulating TNF levels subsequently increased brain levels of TNF, which led to inhibition of the NAD-linked state III respiration rate. The latter is mediated through complex I but not complex II. The anti-TNF antibody prevented the decline in mitochondrial respiration of brain tissues, consistent with this notion.

Pro-survival and pro-apoptotic protein levels in mitochondria

To probe the possibility that ADR induced increased levels of serum and brain TNF are associated with altered levels of pro- and anti-apoptotic proteins in brain mitochondria, the levels of the pro-apoptotic proteins, p53 and Bax, and the anti-apoptotic proteins, Bcl-xL were quantified (Fig. 2.7). The results demonstrate that p53 was increased in mitochondria at early time point 3, 6, 24 h after ADR treatment compared with saline control (*$p<0.01$), then declined at 48, and 72 h. Bax increased with a similar kinetics to that of p53 (*$p<0.01$). The anti-apoptotic protein, Bcl-xL increased after treatment with ADR at 6, 24, 48 and 72 h compared with saline control (*$p<0.05$). The level of succinate dehydrogenase was not changed and was used for normalization protein

loading control. These results demonstrated a rapid increase of pro-apoptotic proteins and anti-apoptotic Bcl-xL in the mitochondria of ADR-treated mice, which are associated with increased TNF in the brain. Consistent with the results shown above, blocking ADR-mediated elevated TNF with anti-TNF antibody resulted in no increase of pro-apoptotic proteins in mitochondria 3 h after treatment with ADR (Fig. 2.8).

p53 forms specific complex with the protective Bcl-xL protein.

p53 can participate in induction of apoptosis by acting directly at the mitochondria (Marchenko et al., 2000; Mihara et al., 2003). Localization of p53 to mitochondria occurs in response to apoptotic signals and precedes cytochrome C release and procaspase-3 activation (Schuler et al., 2001). To determine the ability of p53 to interact with Bcl-xL in brain mitochondria, immunoprecipitation was performed using an antibody to p53 to precipitate mitochondrial proteins, and the complexes were probed with antibodies to p53 and Bcl-xL by Western blot analysis. The results showed specific increases of p53 and Bcl-xL in the ADR treatment groups compared to the controls (Fig. 2.9A, $*p<0.05$). Blocking circulating TNF with anti-TNF antibody resulted in no ADR-mediated increased p53 and Bcl-xL complex in mitochondria (Fig. 2.9B).

Cytochrome c release from the mitochondria to cytosol

We also examined whether ADR treatment led to brain mitochondrial membrane pore opening assessed by cytochrome c release. Cytochrome c release from mitochondria and elevation in cytosol were found in the brain of mice treated with ADR or IgG followed by ADR compared with saline or IgG-treated mice alone ($*p<0.01$). Anti-TNF antibody prevented cytohrome c released from mitochondria to cytosol (Fig. 2.10).

Increased caspase 3 activity and apoptosis

Release of cytochrome c from mitochondria to cytosol induces caspase 3 cleavage and apoptosis in brain tissues. Three hours following treatment of mice with ADR, increased caspase 3 activity was observed in brain tissues (*$p<0.001$). There was a progressive increase in caspase 3 activity after ADR treatment for 72 h (*$p<0.001$, Fig. 2.11). TUNEL-staining demonstrated dark brown nuclear condensation characteristic of apoptotic cell death corresponding to the time point of elevated caspase 3 activity in ADR-treated mice compared with saline control (*$p<0.01$) and are further increased at 72 h compared with 3 h ADR-treated mice (**$p<0.05$, Fig. 2.12).

Discussion

A somnolence syndrome (also known as cognitive dysfunction), which often is called "chemobrain" by cancer patients receiving ADR, has been unexplored, possibly due to the accepted notion that ADR does not pass the blood-brain-barrier. In this report, we confirmed that ADR accumulated only in areas outside the blood brain barrier, but increased TNF levels were found in serum and both the hippocampal and cortical regions of the brain. Mitochondrial function was altered in brain following ADR treatment. Furthermore, a neutralizing antibody against TNF given systemically abolished the observed TNF levels in brain tissue. Our results support the hypothesis that TNF is an important mediator of the observed ADR-induced mitochondrial dysfunction in brain.

Systemic TNF is well recognized to act as a signal in the complex network of immune-neuron interaction, which affects the CNS (Besedovsky et al., 1996; Blattleis et al., 1998; Licinio et al., 1997), such as in HIV and Alzheimer's disease (Eric et al., 2002; Mattson et al., 2005; Valcour et al., 2004; Greig et al., 2004; Pocernich et al., 2005). Our finding that the tissue levels of TNF increase in brain tissue is consistent with the effect of ADR on circulating TNF levels. Circulating TNF may enter the brain by transport across the blood brain barrier and stimulation of local TNF production after physically entering the brain (Gutierrez et al., 1993; Osburg et al., 2002). Alternatively, increased brain TNF levels may result from the activation of microglia and macrophages that enter the brain after ADR treatment. TNF can act on brain cells to cause the observed decline in mitochondrial respiration and subsequent increase in oxidative stress markers (Joshi et al., 2005). This possibility is strongly supported since neutralizing antibody successfully alleviated the decline in mitochondrial respiration of brain tissue after treatment with ADR. Our results are consistent with those previously reported by Usta, et al. (2004), who showed that pentoxiphylline (PTX), an inhibitor of TNF, prevented an ADR-mediated systemic increase in TNF and nephropathy.

Our results indicate that ADR induced a decline in brain mitochondrial respiration complex I, but had no effect on complex II. This is consistent with the possibility that the [4Fe-4S] cluster protein in complex I is inactivated by ROS generated in mitochondria, since the [4Fe-4S] protein of complex I extends into the inner membrane where superoxide is generated. This possibility

is strongly supported by our previous studies, which demonstrated that transgenic mice overexpressing MnSOD are protected from ADR-induced complex I inactivation in cardiac tissues (Yen et al., 1996, 1999). Mitochondrial dysfunction may be one of the signals initiating the mitochondrial apoptosis pathway by translocation of pro-apoptotic proteins, p53 and Bax, to mitochondria, which, in turn, led to cytochrome c release and subsequent induction of caspase 3 cleavage and apoptotic cell death. The increase of these pro-apoptotic proteins coincides with the increase in mitochondrial dysfunction, suggesting mitochondrial dependent tissue injury. Our finding that p53 interacted with Bcl-xL in mitochondria further supports the role of mitochondria in ADR-induced CNS injury. These data are consistent with recent reports demonstrating that Bax is required for p53 translocation to mitochondria (Chipuk et al., 2003, 2004). Our result confirms and extends several recent studies, which demonstrated that p53 can directly induce permeabilization of the outer mitochondrial membrane by forming complexes with the pro-survival, Bcl-xL protein (Marchenko et al., 2000; Mihara et al., 2003; Schuler et al., 2001). The mitochondrial alteration reported in the current study could be involved in the elevated oxidative stress in brain following ADR treatment (Joshi et al., 2005).

p53 protein localizes to the mitochondria by which p53-dependent apoptosis pathway but not during p53-mediated cell cycle arrest. The accumulation of p53 in mitochondria is rapid within 1 hour after p53 activation by cellular stress and precedes changes in mitochondrial membrane potential, cytochrome c release, and procaspase-3 activation (Marchenko et al., 2000). p53 accumulates in the cytoplasm, where it directly regulates the pro-apoptotic protein Bax to promote mitochondrial outer-memebrane permeabilization; Bax then brings p53 to mitochondria (Mihara et al., 2003, Chipuk et al., 2004). Pro-apoptotic protein, p53 also can directly induce permeabilization of outer mitochondrial membrane by forming complexes with Bcl-xL, resulting in cytochrome c release (Mihara et al., 2003). Overexpression of anti-apoptotic protein, Bcl-xL abrogates stress signal-mediated mitochondrial p53 accumulation and apoptosis (Machenko et al., 2000).

Our results support the notion that p53 and Bax are translocated to mitochondria early following with ADR treatment, which is the same kinetics for mitochondrial membrane permeabilization and cytochrome c release-initiated apoptotic cell death. The stabilization of p53 by with interact with Bax prevent p53 degradation by the metalloprotease MDM2 (Tan et al., 2001). In

response to this pro-apoptotic stress, our results suggest that the braib tries to compensate to promote cell survival by increased induction of the anti-apoptotic protein, Bcl-xL, which is increased later at 6 h following ADR treatment.

In summary, our results for the first time provide direct biochemical evidence of ADR toxicity to brain. In particular, our results demonstrate that ADR-induced circulating TNF is causally related to the observed CNS injury associated with this cancer chemotherapeutic agent. TNF-induced mitochondrial dysfunction with its downstream consequence leading to further increases in oxidative stress in the brain may, at least in part, be responsible for the cognitive dysfunction (somnolence syndrome) observed in many patients undergoing ADR-based chemotherapy. Whether ADR-induced circulating TNF is directly responsible for the observed brain mitochondrial dysfunction, or circulating TNF further increased TNF from activated glia cells remains to be determined, but merits further investigation. Our results, which demonstrated that a neutralizing antibody against TNF abolished the observed mitochondrial injury in animals treated with ADR, are highly encouraging, since antibodies against TNF have been in clinical use for many inflammatory associated diseases. Studies to determine if such an approach may be useful to prevent cognitive dysfunction but not inhibit the cancer chemotherapeutic properties of ADR are in progress.

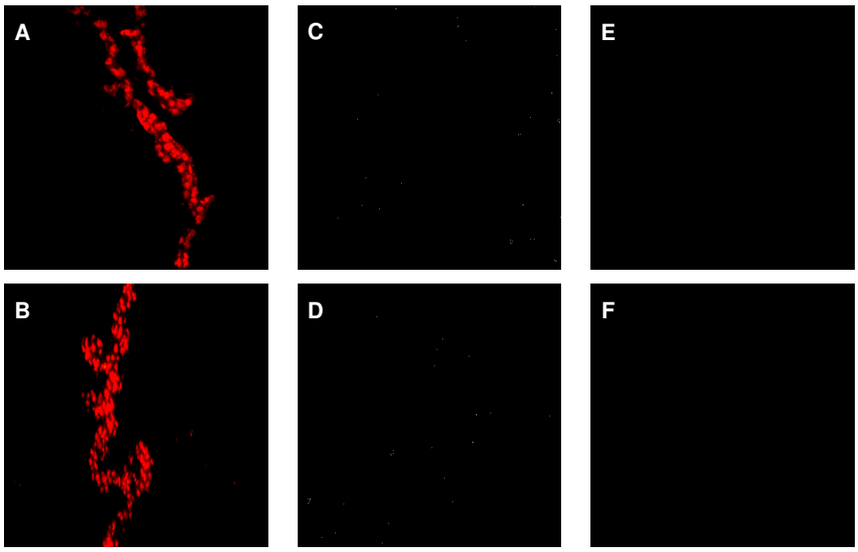

Figure 2.1: Localization of Adriamycin in mouse brain. Adriamycin localization (orange-red fluorescence) in mouse brain 3 h after 20 mg/kg ADR was apparent in the choroid plexus. A, ADR alone; B, anti-TNF antibody immediately followed by ADR; C, Saline; D, anti-TNF antibody alone. The ADR orange-red fluorescence was not detected in cortex (E), and hippocampus (F). Magnification 20x.

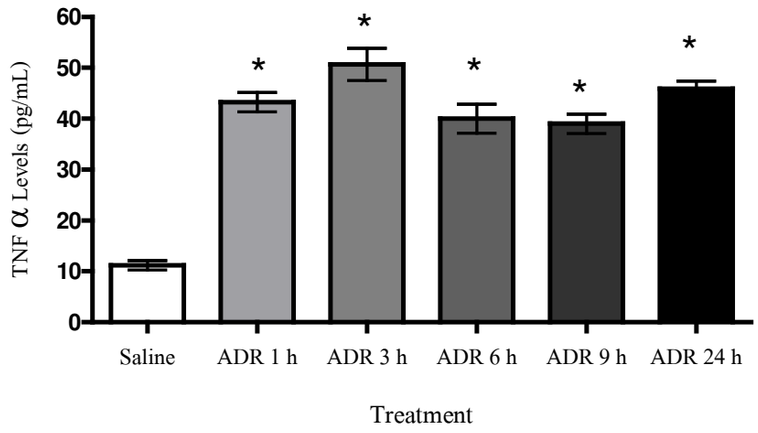

Figure 2.2: Adriamycin increased circulating TNF. TNF levels are significantly elevated in mice 3 h after 20 mg/kg ADR compared with saline control (*$p<0.001$). The levels of TNF were increased at the earliest time point examined.

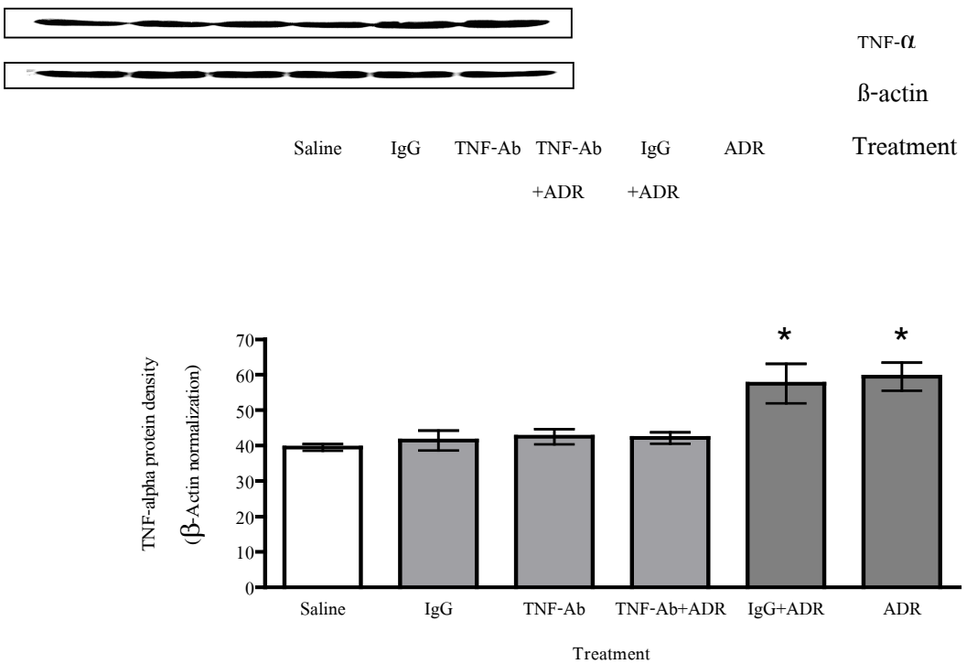

Figure 2.3: Adriamycin-induced TNF is increased in brain tissues. TNF levels were significantly increased in mice 3 h after treatment with a single dose of 20 mg/kg ADR or IgG followed by ADR compared with the saline or IgG control (*$p<0.01$). The levels of TNF were not different in mice treated with anti-TNF antibody (TNF-Ab), immediately followed by ADR. Anti-TNF antibody treatment alone did not increase TNF levels in the brain.

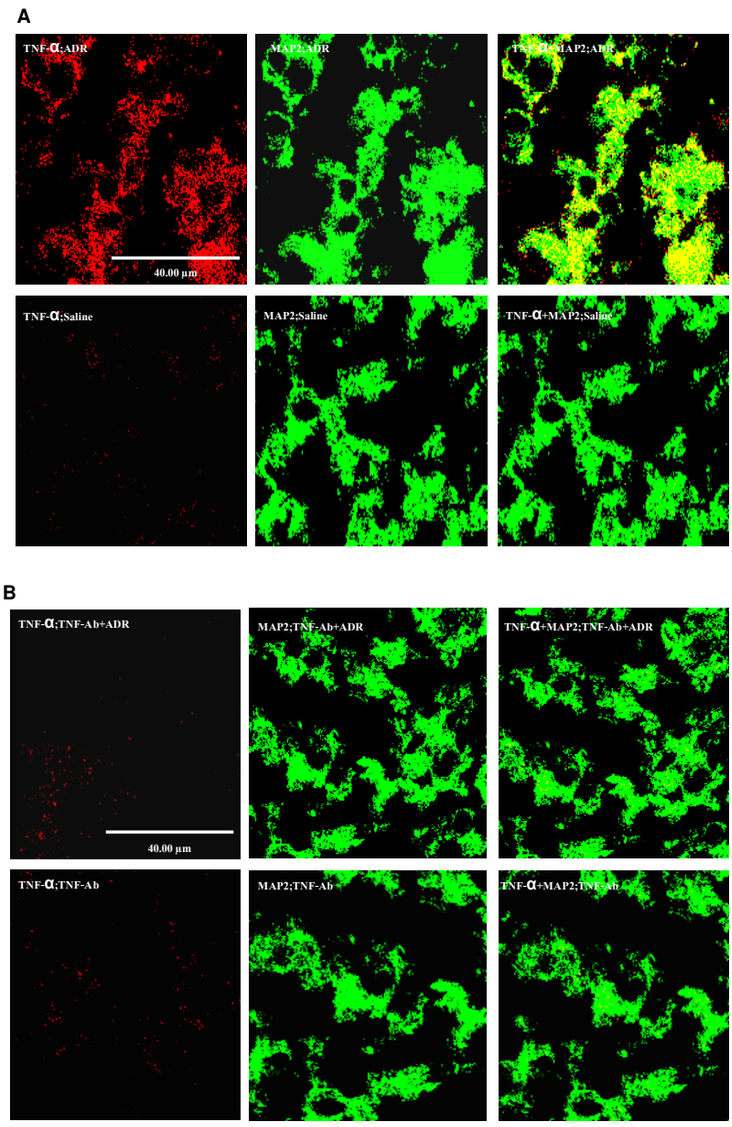

Figure 2.4: Immunofluorescence analysis of TNF localization in cortex following ADR treatment. Confocal microscopy analysis of TNF (red) and neurons (MAP2, green) and colocalization (yellow) showed that TNF is increased in neurons of mice 3 h after treatment with 20 mg/kg ADR compared to mice treated with saline (4A), anti-TNF-antibody together with ADR or anti-TNF antibody alone (4B). Pictures are representative images from at least 3 independent experiments per group.

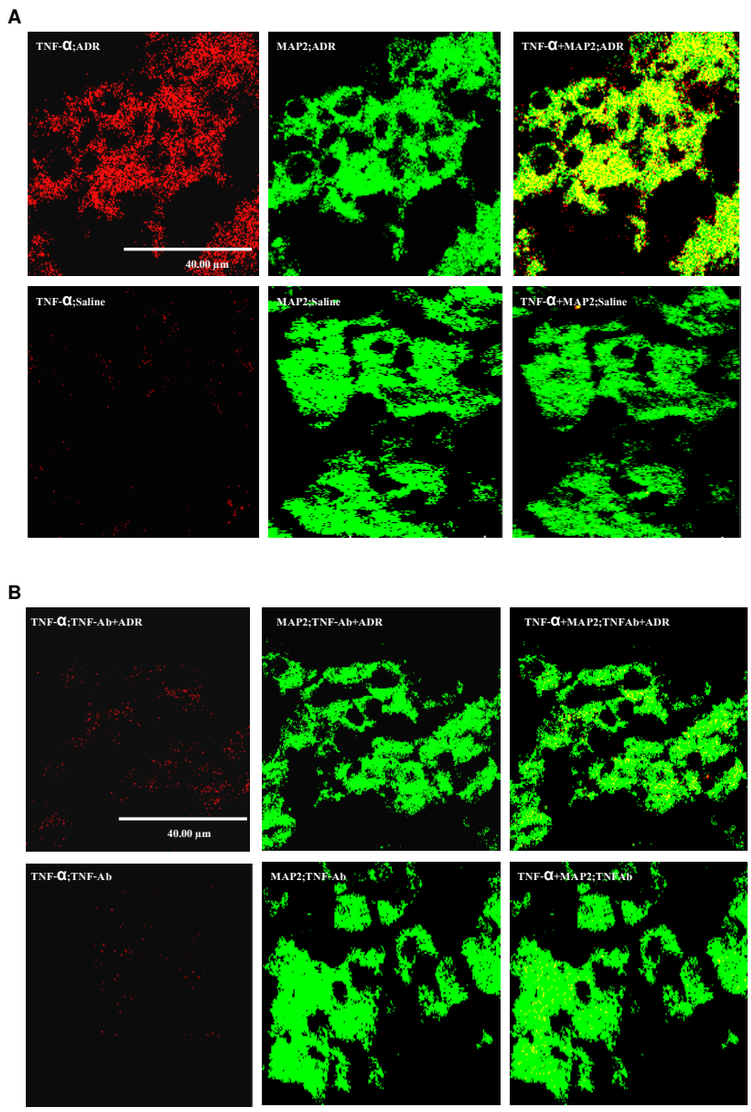

Figure 2.5: Immunofluorescence analysis of TNF localization in hippocampus following ADR treatment. Confocal microscopy analysis of TNF (red) and neurons (MAP2, green) and colocalization (yellow) showed that TNF is increased in neurons of mice 3 h after treatment with 20 mg/kg ADR compared to mice treated with saline (5A), anti-TNF-antibody together with ADR or anti-TNF antibody alone (5B). Pictures are representative images from at least 3 independent experiments per group.

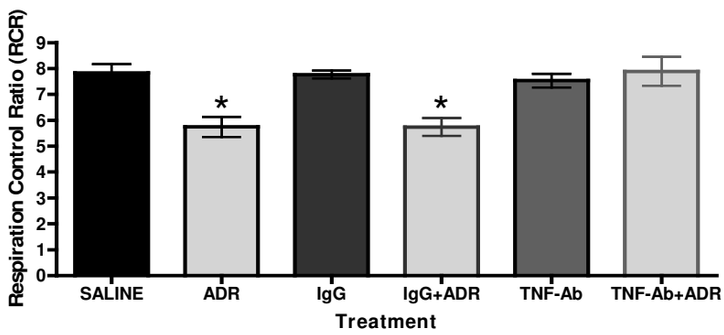

Figure 2.6: Adriamycin-mediated TNF elevation leads to mitochondrial dysfunction. Brain mitochondrial respiration was determined using pyruvate + malate as substrates from isolated intact mitochondria of ADR-treated mice. The results show mitochondrial respiration complex I, pyruvate + malate as substrates, was significantly decreased (* $p < 0.05$ compared to all other groups) 3 h after treatment with ADR or IgG followed by ADR and the mitochondrial respiration decline was blocked by anti-TNF antibody. Data represent the mean + SEM of six independent experiments.

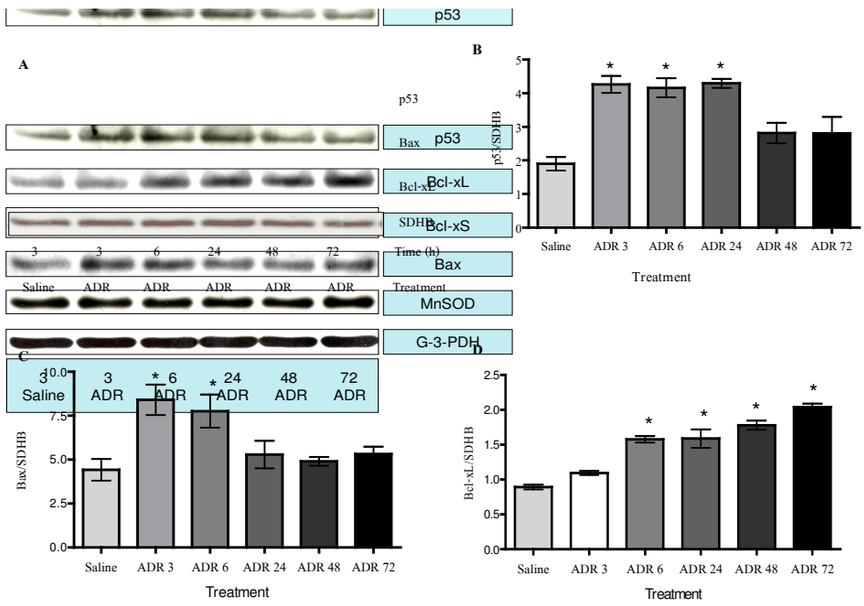

Figure 2.7: Representative immunoblots showing the levels of p53, Bax, Bcl-xL, and succinate dehydrogenase in mitochondria. Mitochondrial proteins were isolated from brain tissues of ADR- and saline-treated mice, and separated by SDS-polyacrylamide gel electrophoresis. The pro-apoptotic proteins, p53 increased at 3, 6 and 24 h (*$p<0.01$) and Bax increased at 3, 6 h (*$p<0.01$) and the anti-apoptotic protein, Bcl-xL show an increase in protein density after treatment with ADR (*$p<0.01$). Succinate dehydrogenase was used to normalize protein loading. The results shown are a representative independent set of data of n = 3 separate sets from individual animals.

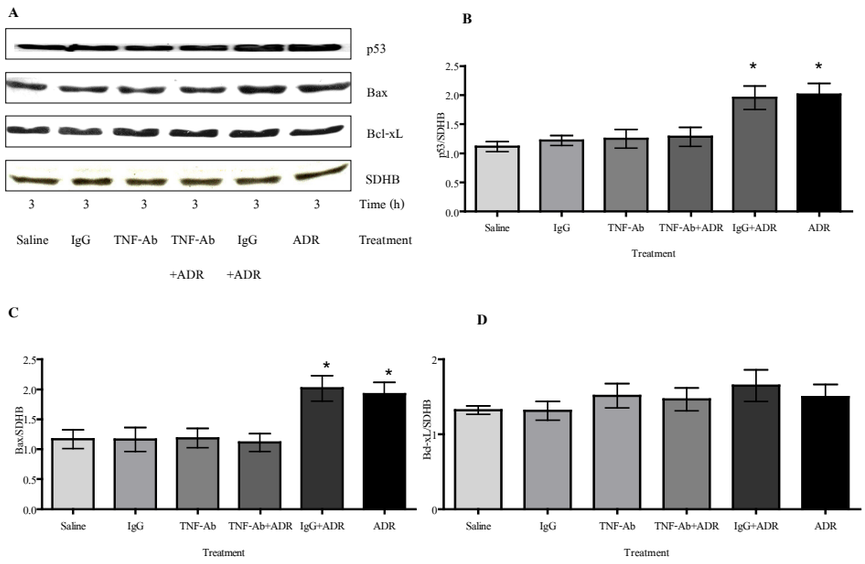

Figure 2.8: Representative immunoblots showing the prevention of p53 and Bax translocation to mitochondria by anti-TNF antibody. Western blot analyses of p53, Bax, Bcl-xL, and succinate dehydrogenase were determined in mitochondrial proteins isolated from brain tissues 3 h after mice were treated with ADR, IgG followed by ADR, anti-TNF antibody immediately followed by ADR, and anti-TNF antibody, IgG or saline as a control. Only the pro-apoptotic proteins, p53 and Bax show an increase in protein density after treatment with ADR or IgG followed by ADR (*$p<0.05$), while no difference in Bcl-xL was observed. Succinate dehydrogenase was used to normalize for protein loading. These results shown are a representative set of data of n = 3 separate sets from individual animals.

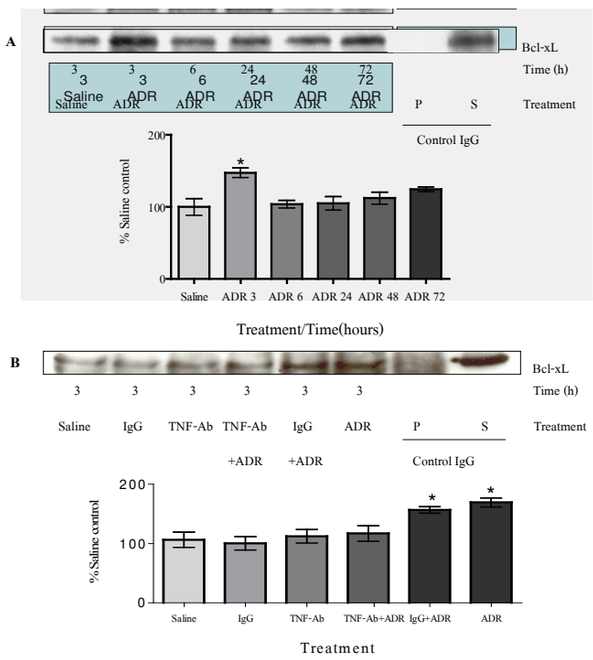

Figure 2.9: Representative co-immunoprecipitation of the anti-apoptotic protein, Bcl-xL, in mitochondria. A, Brain mitochondria were isolated from mice after ADR or saline control treatment, and were immunoprecipitated with anti-p53 antibody and the precipitation probed with antibody to Bcl-xL. Specific bands of Bcl-xL were increased at 3 h (*$p<0.05$). B, Blocking with anti-TNF antibody prevented p53 translocation to mitochondria and co-localization with Bcl-xL in mice 3 h after injection with anti-TNF antibody immediately followed by ADR compared to mice treated with ADR or IgG followed by ADR (*$p<0.05$). IgG; pre-immune serum. Pellet, isolated mitochondrial protein was used to immunoprecipitate by IgG and analysis of the pellet by Western blo using antibody against Bcl-xL showed no band, but the supernatant showed a band. The results are shown a representative set of data of n = 3 separate sets from individual animals.

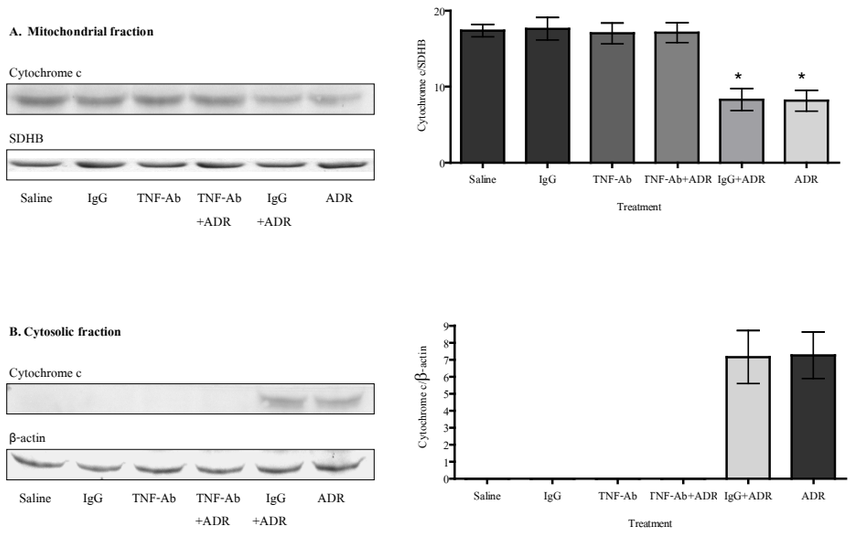

Figure 2.10: ADR induced cytochrome c released from mitochondria to cytosol. Western blot analyses of cytochrome c and succinate dehydrogenase or β-actin were determined in mitochondrial or cytosolic fraction isolated from brain tissues 3 h after mice were treated with ADR, IgG followed by ADR, anti-TNF antibody immediately followed by ADR, and anti-TNF antibody, IgG or saline as a control. Cytochrome c was decreased in mitochondria (*$p<0.01$) but increased in cytosol after treatment with ADR or IgG followed by ADR. Succinate dehydrogenase or β-actin were used to normalize for protein loading. These results shown are a representative set of data of n = 3 separate sets from individual animals.

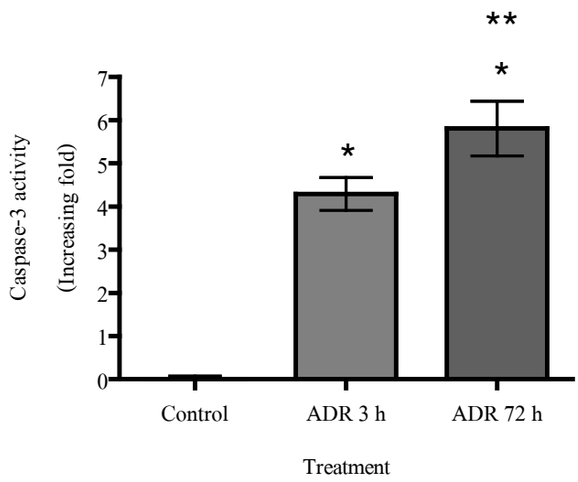

Figure 2.11: ADR-induced caspase 3 activity in brain tissues. Caspase 3 activity is significantly increased in mice 3 and 72 h following ADR treatment compared with saline control (*$p<0.001$) and also increased at 72 h compared with 3 h after 20 mg/kg ADR (**$p<0.05$). These results shown are a representative set of data of n = 3 separate sets from individual animals.

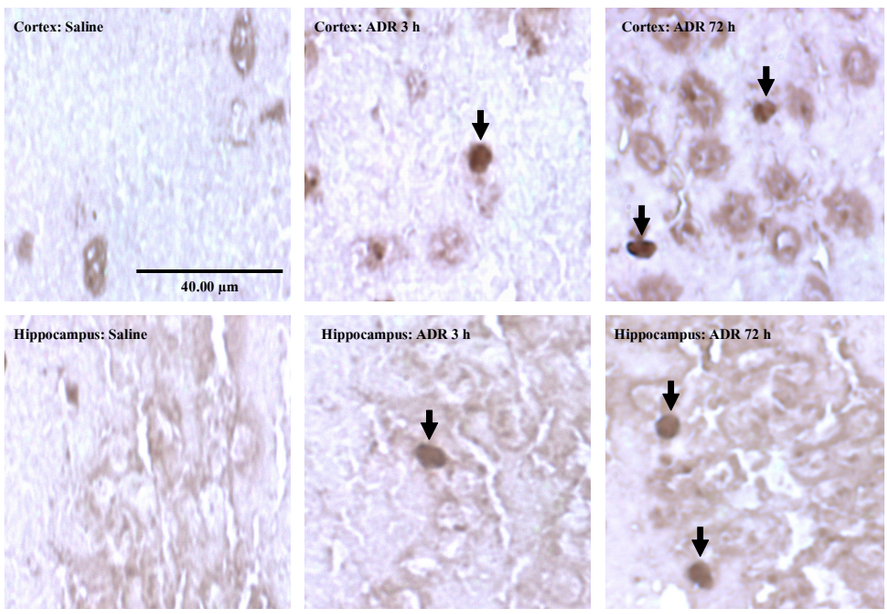

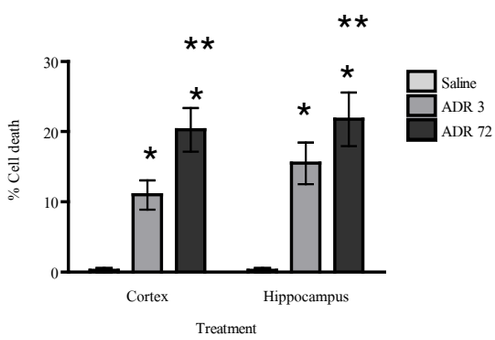

Figure 2.12: ADR-induced TUNEL positive apoptotic cell death in cortical and hippocampal regions of the brain. Brain cryosection tissues were treated with biotinylated rTdT, followed by streptavidin peroxidase and diaminobenzidine-hydrogen peroxide, and counterstained with methyl-green. The nuclei are represented by the positive dark brown staining. Following 3 h and 72 h after ADR treatment an increased number of apoptotic cells were found in cortical and hippocampal cells compared with saline (*$p<0.01$) and the apoptotic cell death further increased at 72 h compared with 3h ADR-treated mice (**$p<0.05$).